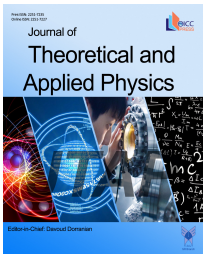

Volume 17, Issue 5, 172346 (1-8)

Journal of Theoretical and Applied Physics (JTAP)

https://dx.doi.org/10.57647/j.jtap.2023.1705.46

Role of dust and ionization on gradient driven instability in a cross-field plasma

Dimple Sharma[1], Munish[2]*, Rajat Dhawan[3], Ravinder Kumar[4]

[1]*Shri Ramdeobaba College of Engineering and Management Nagpur, Maharashtra, India.*
[2]*Department of Physics, Gargi College, University of Delhi, Delhi, India.*
[3]*Department of Physics, MM Engineering College, Maharishi Markandeshwar, Mullana-Ambala, Haryana, India.*
[4]*Department of Physics, Janta Vedic College Baraut, Uttar Pradesh, India.*

***Corresponding author**: munishiitkgp@gmail.com

Received 24 April 2023; Accepted 08 July 2023; Published Online 13 July 2023 ORIGINAL RESEARCH

Abstract:
Presence of dust in cross-field plasma systems such as Hall thrusters or in plasma processing units changes the whole physical phenomenon. Owing to the density gradient, pressure gradient and spatial variation of the magnetic field, the plasma in these devices is often found to be unstable and hence, instability evolves in these systems. Considering dust contamination and ionization in the plasma, we make theoretical study on the growth rate of the instability under the effect of dust density, dust mass and dust charge in addition to the effect of ion temperature, ion temperature gradient, scale length of density inhomogeneity and profile of the ion velocity. For their effective use, the said plasma systems need to be instability free, and the model developed in the present article will help experimentalists to optimize the plasma parameters, external magnetic field and biasing voltage.

Keywords: Cross-field plasma; Plasma processing; Dust contamination; Film deposition; Plasma etching; Thruster plasmas; Growth rate; Perturbed potential

1. Introduction

Atmospheric pressure plasma-enhanced chemical vapour deposition (AP-PECVD) is a technique to deposit thin films from a gas state (vapour) to a solid state on a substrate. Although AP-PECVD technique produces good-quality semiconductor or insulator thin films, still the reports on these techniques are very feeble. It may happen as the high collision frequency in atmospheric plasma provokes large secondary ionization in the gas phase to generate dust particles which eventually degrades the film quality, resulting in poor uniformity of the film [1]. Plasma etching is performed to make via-holes and during this process dust is generated [2–5]. During this process number of particles including dust behave differently and are categorised according to their velocities [6]. Sometimes the walls are coated with thin films inside the chamber which is called as wall conditioning; but due to series of discharges taking place inside the chamber degrades it, making it weak and flaky, which eventually releases the flaky dust matter which levitates inside the chamber. Due to electrostatic charging and magnetic effects this dust matter may get charged positively or negatively [7]. Inductively coupled plasmas (ICPs) are extensively used for materials processing and microelectronics fabrication [8–10]. During this processing many impurities are also produced as by product which is called as dust. On the other hand, in fusion devices, the dust particles are released by collisions of plasma species with the chamber walls because of erosion. Such dust particles are charged ions which hinder the motion of electrons in the chamber. Hence, the study of dust and its parameters to prevent the fusion devices from the possible degradation is very important [11].

$\mathbf{E} \times \mathbf{B}$ systems are of huge importance as the Hall thrusters are primarily used in earth orbiting satellites and space robotics aircrafts. The dust can also attain charge on the surface of supersonically moving aircraft [12–14], leading to the formation of plasma. The improved efficiency and large thrust densities of thrusters are attracting the scientific fraternity to use them for various other space applications [15,16]. However, the plasma used in these devices stay unstable due to the gradients in plasma density and magnetic field [17,18].

Also due to collision, the azimuthal propagating waves can couple with the electron drift and grow with time. Such mechanism leads to the growth of the instabilities [19]. High frequency instabilities have been studied by Lazurenko et al. and they found that the instabilities are higher in the exit region of the thrusters [20]. Theoretical model has been presented by Kapulkin and Guelman for analysing low frequency instabilities and they observed that non-uniform plasma and magnetic field both are responsible for these instabilities [21]. Low frequency oscillations inside the thruster chamber under the impact of ionization have also been studied by the Barral et al. [22]. Chable and Roguier [23] described Buneman's instability arising from low frequency oscillations because of coupling between self-consistent electric field and the ion. Chesta et al. [24] and Parker et al. [25] found a completely different type of instability named as rotating spoke instability in annular Hall thrusters. Further Frias et al. [26] and Smolyakov et al. [27] reported the long-wavelength gradient drift instabilities, but they neglected the electron inertia effect. Starodubtsev et al. [28] have investigated low-frequency sheath instability in non-Maxwellian plasmas.

The mechanism of thrust generation in cross-field ($\mathbf{E}\times\mathbf{B}$) systems or Hall thrusters is disturbed due to instabilities. Hence, recently, a focus has evolved on the magnetic field profile for achieving a controlled divergence of the plasma plume responsible for the thrust in such devices including magnetic nozzle [29]. Particular magnetic field profile and density/pressure variation has been found to enhance the thrust and efficiency [30–32]. Not only this, the magnetic field is found to play an important role in other fields of radiation as well [33]. The dust has been found to influence the Rayleigh-Taylor instability [34, 35] and resistive instability [36] in the Hall thruster channel. The position of dust whether inside or outside the channel is also shown to significantly alter the instabilities. However, these findings concern the Hall thruster plasmas where only the electrons are magnetized. It would be of much interest to examine whether the influence of the dust remains the same on the growth rate of the instability when both the plasma species, i.e., the ions and the electrons, are magnetized, means in any $\mathbf{E}\times\mathbf{B}$ systems used in plasma processing. Since continuous ionization also takes place in the plasma processing systems, this is necessary to include the ionization in the mathematical modelling. Hence, this article focuses on the gradient driven instability under the impact of dust contamination and the ionization in an $\mathbf{E}\times\mathbf{B}$ system.

2. Theoretical plasma model

In the present study, the magnetic field is applied ($\mathbf{B}$) in the z-direction due to which both the species, i.e. ions and electrons, are assumed to be magnetized. As both ions and electrons have finite temperature, a non-zero pressure-gradient term will exist, which is taken in to account through their respective fluid equations. We consider n_j as the density, T_j as the temperature and m_j as the mass of the electrons ($j=e$) and ions ($j=i$). U and V, are taken as velocities of the electrons and the ions. e and Ze are the charges of the electrons and ions. The un-perturbed and oscillating part of densities are represented by (n_{i0},n_{e0}) and (n_{i1},n_{e1}) and those of velocity components as $(V_{x0},U_{x0},V_{y0},U_{y0})$ and $(V_{x1},U_{x1},V_{y1},U_{y1})$. The perturbed potential and electric field are φ_1 and $\mathbf{E}_1$.

The basic fluid equations, such as continuity equation and equation of motion, are used for the ion fluid, electron fluid and dust fluid, whose linearized form is written below.

$$\partial_t n_{e1}+n_{e0}\partial_x U_{x1}+n_{e0}\partial_y U_{y1}+U_{x1}\partial_x n_{e0}+U_{y0}\partial_y n_{e1}=\alpha n_{e0}+\alpha n_{e1} \tag{1}$$

$$\partial_t U_{x1}+U_{y0}\cdot\partial_y U_{x1}=\frac{e}{m_e}\cdot\partial_x\varphi_1-\frac{e}{m_e}\cdot(U_{y0}+U_{y1})(B_0)-\frac{2T_e}{m_e n_e}\cdot\partial_x n_{e0}-\frac{2T_e}{m_e n_e}\cdot\partial_x n_{e1}-\frac{2}{m_e}\partial_x T_e-\alpha U_{x1} \tag{2}$$

$$\partial_t U_{y1}+U_{x1}\cdot\partial_x U_{y0}+U_{y0}\cdot\partial_y U_{y1}=\Omega_e U_{x1}-\frac{2T_e}{m_e n_e}\cdot\partial_y n_{e1}+\frac{e}{m_e}\cdot\partial_y\varphi_1-\alpha U_{y0}-\alpha U_{y1} \tag{3}$$

$$\partial_t n_{i1}+n_{i0}\partial_x V_{x1}+V_{x1}\partial_x n_{i0}+n_{i0}\partial_y V_{y1}+V_{y0}\partial_y n_{i1}=\alpha n_{i0}+\alpha n_{i1} \tag{4}$$

$$\partial_t V_{x1}+V_{y0}\partial_y V_{x1}=-\frac{Ze}{m_i}\partial_x\varphi_1+\frac{Ze}{m_i}\cdot(V_{y0}+V_{y1})(B_0)-\frac{2T_i}{m_i n_i}\cdot(\partial_x n_{i0}+\partial_x n_{i1})-\frac{2}{m_i}\partial_x T_i-\alpha V_{x1} \tag{5}$$

$$\partial_t V_{y1}+V_{x1}\partial_x V_{y0}+V_{y0}\partial_y V_{y1}=-\frac{Ze}{m_i}\cdot\partial_y\varphi_1-\frac{Ze}{m_i}\cdot V_{x1}(B_0)-\frac{2T_i}{m_i n_i}\cdot\partial_y n_{i1}-\alpha V_{y0}-\alpha v_{y1} \tag{6}$$

$$\partial_t n_{d1}+\mathrm{v}_{d0}\partial_x n_{d0}+\mathrm{v}_{d1x}\partial_x n_{d0}+\mathrm{v}_{d0}\partial_x n_{d1}+n_{d0}(\boldsymbol{\nabla}\cdot\mathbf{v}_{d1})=0 \tag{7}$$

$$\partial_t \mathrm{v}_{d1}+\mathrm{v}_{d0}\partial_x \upsilon_{d1}=\frac{eZ_d}{m_d}E_1-\frac{\boldsymbol{\nabla}p_d}{m_d n_{d0}} \tag{8}$$

In Eqs. (1)-(8), ∂_t, ∂_x and ∂_y are the first-order derivatives with respect to time, x and y, respectively. α is the ionization frequency. We consider $\Omega_i=eB_0/m_i$ and $\Omega_e=eB_0/m_e$ as the ion-cyclotron and electron-cyclotron frequencies, respectively, $\acute{A}=i\omega-\alpha-ikU_{y0}$ and $\acute{B}=1+(2T_e k^2)/(\acute{A}m_e\omega)$ with k is the wavenumber corresponding to the oscillations of the wavelength λ. $A_1=i\omega-\alpha-ikV_{y0}$ and $B_1=1+(2T_i k^2)/(A_1 m_i\omega)$. ω_i is the ion-plasma frequency, given by $(n_{i0}e^2/m_i\varepsilon_0)^{1/2}$ and ω_e is the electron-plasma frequency, given by $(n_{e0}e^2/m_e\varepsilon_0)^{1/2}$.

Poisson's equation which reveals the relationship between plasma species densities and the electric potential is stated as follows

$$\varepsilon_0(\partial_x^2+\partial_y^2)\varphi_1=e(n_{e1}-Zn_{i1}+Z_d n_{d1}). \tag{9}$$

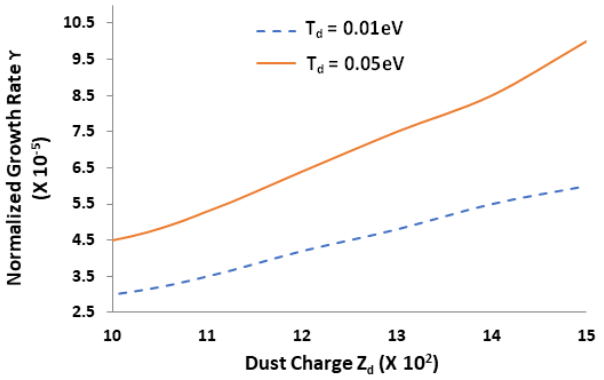

Figure 1. Normalized growth rate of instability as a function of dust charge for different temperature of dust (T_d) in eV, when $d = 5$ m, $\lambda = 5$ cm, $x = \lambda/4$, $n_{i00} = 10^{18}$ m^{-3}, $n_{d0} = 5 \times 10^{11}$ m^{-3}, $T_i = 0.3$ eV, $m_i = 1.6 \times 10^{-27}$ kg, $V_{y00} = 10^3$ m/s, $U_{y00} = 10^5$ m/s, $Z = 1$, $\alpha = 10^2$ s^{-1} and $dT_i/dx = 1$ eV/m.

After putting the expressions of the perturbed densities of the ions, electrons and dust in the above equation, we get

$$(\partial_x^2\varphi_1 - \mathrm{k}^2\phi_1) + \partial_x^2\varphi_1\left[\frac{n_{e0}e^2}{X_1\acute{A}\acute{B}\varepsilon_0 m_e\omega_e} - \frac{Z^2e^2n_{i0}}{S_1A_1B_1m_i\omega_i\varepsilon_0} - \frac{Z_d^2e^2n_{d0}}{\varepsilon_0(M_d\omega^2 - \gamma_dT_dk_y^2)}\right] + \mathrm{k}^2\phi_1\left(\frac{Z^2e^2n_{i0}\omega_i}{A_1B_1m_i\Omega_i^2\varepsilon_0} + \frac{Z_d^2e^2n_{d0}}{\varepsilon_0(M_d\omega^2 - \gamma_dT_dk_y^2)}\right) + \phi_1\left[\frac{Zei\mathrm{k}P_1\omega_i}{Q_1m_i\Omega_i^2} - \frac{i\mathrm{k}T_1\omega_ee}{U_1m_e\Omega_e^2} + \frac{V_1e^2B_0i\mathrm{k}}{W_1X_1m_e^2\omega_e}\right] + \left[-\frac{\alpha n_{e0}e}{\acute{A}\acute{B}\varepsilon_0} + \frac{Ze\alpha n_{i0}}{A_1B_1\varepsilon_0} - \frac{2T_iP_1}{Q_1m_in_{i0}\Omega_i}\partial_xn_{i0} - \frac{2P_1}{Q_1m_i\Omega_i}\partial_xT_i - \frac{2T_iP_1ZeB_0}{Q_1m_i^2\Omega_i^2n_{i0}}\partial_xn_{i0} - \frac{2P_1ZeB_0}{Q_1m_i^2\Omega_i^2}\partial_xT_i + \frac{2T_iZei\mathrm{k}}{A_1B_1m_i\Omega_i\varepsilon_0}\partial_xn_{i0} + \frac{2i\mathrm{k}n_{i0}Ze}{A_1B_1m_i\Omega_i\varepsilon_0}\partial_xT_i + \frac{2i\mathrm{k}Z^2e^2T_iB_0}{A_1B_1m_i^2\Omega_i^2\varepsilon_0}\partial_xn_{i0} + \frac{2i\mathrm{k}Z^2e^2n_{i0}B_0}{A_1B_1m_i^2\Omega_i^2\varepsilon_0}\partial_xT_i + \frac{2i\mathrm{k}n_{i0}Ze}{A_1B_1m_i\Omega_i^2\varepsilon_0}\partial_xT_i\partial_xV_{y0} + \frac{2R_1KT_i}{S_1^2en_{i0}}\partial_xn_{i0} + \frac{2V_1T_e}{W_1X_1m_en_{e0}\omega_e}\partial_xn_{e0} - \frac{2P_1T_i i\mathrm{k}\omega_i}{Q_1m_i\Omega_i^2} + \frac{2V_1T_ei\mathrm{k}B_0e}{W_1X_1m_e^2\omega_e^2} + \frac{eZ_d^2\gamma_dT_d}{\varepsilon_0(M_d\omega^2 - \gamma_dT_dk_y^2)}\partial_x^2n_{d0}\right] = 0. \tag{10}$$

The coefficients used in the above equation are given in Appendix.

Considering the ionization to take place in one end of the chamber of plasma devices, we take $S_0 = S_{00}\exp[-10(x/d)^2]$ kind of variation of the ion and the electron densities, and also their velocities, we take the peak values as n_{e00}, n_{i00}, n_{d00}, U_{i00} and V_{i00}. Clearly the width of the distribution enhances with the value of d, meaning the spatial variation of the said quantity is slow for larger values of d and hence, a wreaker gradient exists in that case. These profiles of velocities and densities are used in Eq. (10), the un-perturbed part of which yields following dispersion equation

$$G_1\omega^6 + G_2\omega^5 + G_3\omega^4 + G_4\omega^3 + G_5\omega^2 + G_6\omega + G_7 = 0. \tag{11}$$

The coefficients and the constants used in Eq. (11) are shown in Appendix.

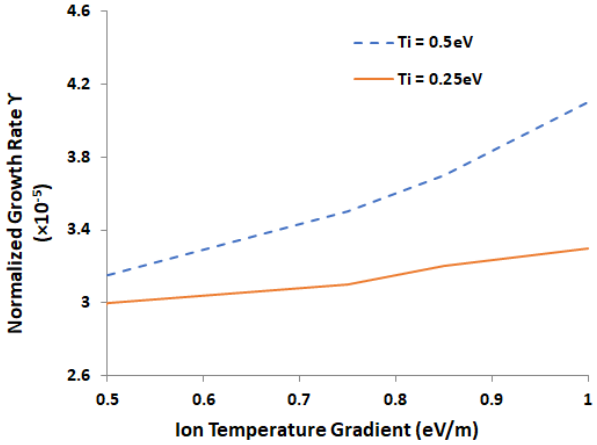

Figure 2. Variation of normalized growth rate of instability with the ion temperature gradient (in eV/m) for different temperature of ions (T_i) in eV, when $d = 5$ m, $\lambda = 5$ cm, $x = \lambda//4$, $n_{d0} = 5 \times 10^{11}$ m^{-3}, $n_{i00} = 10^{18}$ m^{-3}, $T_e = 1.5$ eV, $m_i = 1.6 \times 10^{-27}$ kg, $V_{y00} = 10^3$ m/s, $U_{y00} = 10^5$ m/s, $B_0 = 1$ T, $M_d = 10^{-23}$ kg, $\alpha = 10^2$ s^{-1} and $Z = 1$.

3. Results and their explanation

Figures 1-5 show the variation of growth rate of instability with different parameters of the dust, ions and electrons. These results are obtained based on the numerical solution [12, 14, 37, 38] of the dispersion Equation (11). The normalized frequency is plotted for discussing the growth rate of the instability.

It is observed from Fig. 1 that the normalized growth rate increases with the increase in dust charge. This can be attributed to the increased Coulomb's force with increase in magnitude of dust charge, leading to instability inside the chamber. Further, increase in the dust temperature also increases the growth rate of instabilities as high temperature produces increased thermal motion and hence it impacts in the same fashion as the large pressure gradient force does. Also, it can be said that this acts in the same manner as strong density gradients in the plasma. Since the cause of this instability is the density gradient, instability of higher growth rate is realized in the chamber. These results on the dust temperature and dust charge are similar effects as obtained by Malik et al. [34] in a Hall thruster plasma when the dust exits in the exit region.

From Fig. 2 it is observed that the growth rate of the instability increases with the ion temperature gradient considered at the scale length much lower than the dimension of chamber. A peculiar trend has also been observed that at low ion temperature gradient temperature of ions doesn't affect

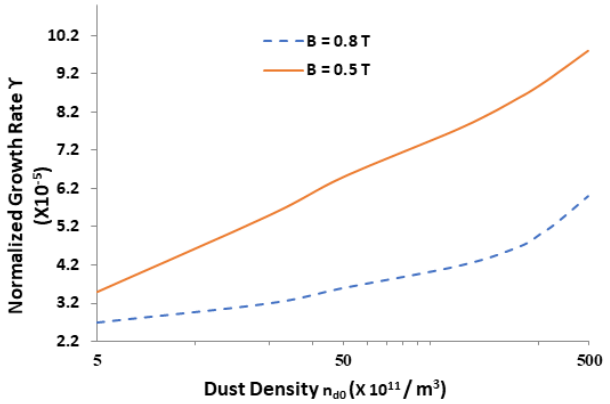

Figure 3. Variation of normalized growth rate of instability with the dust density (in /m3) for different values of magnetic field (in Tesla), when $d = 5$ m, $\lambda = 5$ cm, $x = \lambda/4$, $n_{i00} = 10^{18}$ m^{-3}, $T_i = 0.3$ eV, $m_i = 1.6 \times 10^{-27}$ kg, $V_{y00} = 10^3$ m/s, $U_{y00} = 10^5$ m/s, $Z_d = 1000$, $Z = 1$, $\alpha = 10^2$ s^{-1}, $M_d = 10^{-23}$ kg, and $dT_i/dx = 1$ eV/m.

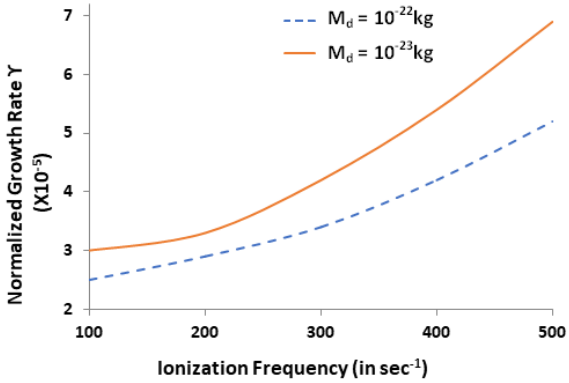

Figure 4. Normalized growth rate of instability as a function of ionization frequency (in sec^{-1}) for different mass of dust when $d = 5$ m, $\lambda = 5$ cm, $x = \lambda/4$, $n_{i00} = 10^{18}$ m^{-3}, $n_{d0} = 5 \times 10^{11}$ m^{-3}, $T_i = 0.3$ eV, $T_e = 1.5$ eV, $m_i = 1.6 \times 10^{-27}$ kg, $V_{y00} = 10^3$ m/s, $U_{y00} = 10^5$ m/s, $B = 1$ T and $dT_i/dx = 1$ eV/m.

the growth rate but at high value of ion temperature gradient as the temperature of ions affects the growth rate of instability. The reason of the enhanced growth rate with the temperature gradient is the same as that of the density gradient. This result is consistent to the case of plasma without dust [39, 40]. This can be seen from Fig. 2 that for the lower values of the temperature gradient the growth rate of the instability is finite but lower. Moreover, a finite value of the growth rate is observed while calculated the growth rate numerically after neglecting the temperature gradient, confirming that the instability occurring in the present case is driven mainly by the density gradient.

The range of dust density is quite large, as the presence of dust also varies largely inside the chamber. Usually inside the chamber the dust density is small and towards the exit plane it is large. It is observed from Fig. 3 that the growth rate of the instability increases as the dust density increases. It is decreased in the presence of stronger magnetic field. This is due to the fact that the oscillation band range of the said instability widen and hence the probability of instabilities lying in the range increases and hence the growth increases. The result on the reduction of the growth rate with stronger magnetic field is the same as observed by other investigators in a Hall thruster plasma [17, 18, 34–36].

The behaviour of normalized growth rate of instability for the ionization frequency has been analysed through Fig. 4 for different values of mass of dust. As ionization becomes larger, the instability grows faster. Also, it is observed that for lighter dust, the instability grows even more sharper and at a higher rate for the larger ionization. This may be because of large Coulomb force. The enhanced growth rate with the ionization frequency is in agreement with the results obtained by other researchers in dust free plasma [17, 18, 39, 40]. The impact of dust mass on the instability in an $\mathbf{E} \times \mathbf{B}$ system is similar results as obtained for the resistive instabilities in the Hall thruster plasmas where only electrons are magnetized [19, 36]. On the other hand, the effect of the dust size can be understood based on the mass of the dust particles. Since the higher mass particles are expected to be larger in size, instability is expected to grow slowly in the presence of dust of the larger size.

Variation of normalized growth rate of instabilities with plasma background density (in m^{-3}) has been shown in Fig. 5 for different values of x and dust densities. It is observed that the magnitude of the normalized growth rate decreases with the increase in the plasma density and it further decreases slightly as the x value is increased. As we know that there is a density gradient present in the plasma which also affects the growth rate of instability. It is observed that instability grows slowly in high plasma density regions than at less density regions. If we talk in terms of wavelength, the growth rate is higher at $x = \lambda/4$ than at $x = \lambda/2$, due to difference in plasma densities at these regions. Further, it is observed that as the dust density increases instability grows at much higher rate. There is a huge difference in the magnitude of the growth rate in the presence of large density of the dust.

If we focus on the above results, we realize that the magnetic field suppresses the instability. In the present calculations, we have considered a uniform magnetic field in the channel, but in reality this field also varies with space and hence one should take into account its spatial variation. Hence, this work can be extended considering the magnetic field profile similar to the field taken in other nonlinear phenomena [41–43]. Then the focus can be given to the effect of field inhomogeneity [32, 44] on the perturbed potential associated with the unstable wave and the growth to the instability. Also, considering weakly relativistic effects of the plasma species will be another interesting problem [45–47]. Moreover, the charge of the dust can fluctuate due to the finite electron and ion currents flowing in or out of the dust particles. The currents develop due to the difference in plasma potential and dust grain surface potential. Other processes such as secondary emission and photoemission of electrons may also take place during the charging [48, 49]

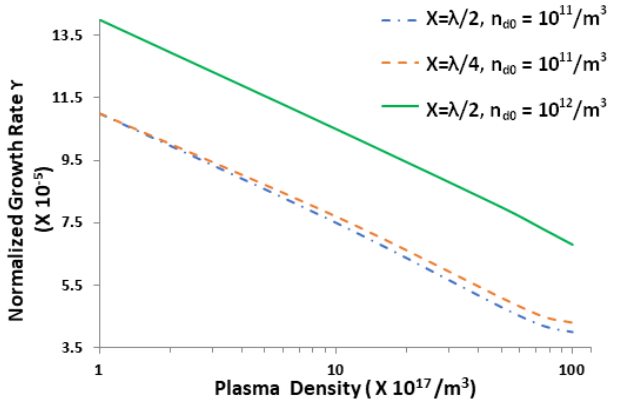

Figure 5. Variation of normalized growth rate of instability with the plasma density (in m^{-3}) for different values of x and dust density, when $d = 5$ m, $\lambda = 5$ cm, $T_i = 0.3$ eV, $T_e = 1.5$ eV, $m_i = 1.6 \times 10^{-27}$ Kg, $V_{y00} = 10^3$ m/s, $U_{y00} = 10^5$ m/s, $B = 1$ T, $\alpha = 10^2$ s^{-1}, $n_{d0} = 5 \times 10^{11}$ m^{-3}, $Z_d = 1000$, $Z = 1$ and $dT_i/dx = 1$ eV/m.

and hence, dust charge fluctuations should be considered.

Finally, this is mentioned that there are a large number of coefficients in the calculations and hence, this is difficult to follow and confirm the correctness. Hence, we discuss the limiting cases by removing the dust particles and ionization from the system, i.e., by neglecting the dust charge Z_d, dust density n_{d0}, dust temperature T_d, and symbol α from the mathematical expressions. Then, the term $2T_d k_d^2 n_{d0}$ from the coefficient F, the term $(2Z_d e k_d n_{d0})/(\omega B_d \varepsilon_0)$ from the coefficient P_1, the term $(k n_{d0} Z_d e)/(\omega B_d \varepsilon_0)$ from the coefficient T_1, the term $(2Z_d e k_d n_{d0})/\varepsilon_0$ from Λ and the term $(2T_d kd)/(m_d \varepsilon_0)\partial_x n_{d0}$ from the coefficient P disappear. Not only this, the coefficient R vanishes in the absence of ionization, the coefficients $\acute{A}$, B_1, D, C, B, H, K, N do not carry the term α, the term $\alpha i m_e n_{e0} \Omega_e^2$ disappears from the coefficient G, the term $(2T_e k^2 \alpha)/(m_e \Omega_e^2)$ disappears from the coefficient K and the term $\alpha D m_e n_{e0} \Omega_e^2$ disappears from the coefficient H. Under the said situation (neglecting either dust or ionization), all the coefficients take the form as obtained in corresponding Refs. [39] and [40]. The coefficients mentioned here alter the growth rate significantly, which is clear when the present results are compared with the results of Refs. [39] and [40]. For example, the growth rate remains lower in the dust free environment. The results are reproduced when we neglect the ionization α, dust density n_{d0}, dust temperature T_d and dust charge Z_d during the numerical calculations. Not only this, but the same results are also obtained when these are not considered in the mathematical expressions and a new dispersion equation is derived and solved. This exercise confirms the correctness of the present calculations.

4. Conclusion

The $\mathbf{E} \times \mathbf{B}$ plasma system having dust contamination and continuous ionization was investigated for gradient driven instability. The normalized growth rate of the instability was found to increase with the increased dust density, dust charge, ion temperature gradient, ionization frequency, whereas the growth was found to reduce in the presence of higher mass of the dust and increased plasma background density. These results will help experimentalists to set up the experiments where the instability can be suppressed and better results are obtained with regard to the plasma processing.

Appendix

The coefficients and the constants used in Eqs. (10) and (11) are given as:

$$P_1 = 3 + \frac{Z^2 e^2 i k n_{i0} B_0}{A_1 B_1 m_i \Omega_i^2 \varepsilon_0} \partial_x V_{y0} + \frac{2 Z_d e k_d n_{do}}{\omega B_d \varepsilon_0},$$
$$Q_1 = 4 + \frac{ZeB_0}{m_i \Omega_i^2} \partial_x V_{y0},$$
$$R_1 = \frac{\Omega_i}{\omega_i^2} \partial_x^2 V_{y0} + \frac{ZeB_0}{m_i \omega_i^2} \partial_x^2 V_{y0},$$

$$S_1 = 1 + \frac{\Omega_i^2}{\omega_i^2} + \frac{2ZeB_0\Omega_i}{m_i \omega_i^2} + 2\frac{\Omega_i}{\omega_i^2} \partial_x V_{y0} + \frac{Z^2 e^2 B_0^2}{m_i^2 \omega_i^2},$$
$$T_1 = \frac{i k n_{e0} e^2 B_0}{\acute{A}\acute{B} m_e \Omega_e^2 \varepsilon_0} \partial_x U_{y0} + \frac{3 i k n_{e0} e}{\acute{A}\acute{B}\varepsilon_0} + \frac{k n_{d0} Z_d e}{\omega B_d \varepsilon_0},$$
$$U_1 = 1 - \frac{eB_0}{m_e \Omega_e^2} \partial_x U_{y0} + \frac{2eB_0}{m_e \Omega_e},$$

$$V_1 = \frac{n_{e0} e \Omega_e}{\acute{A}\acute{B}\varepsilon_0 \omega_e^2} \partial_x^2 U_{y0} + \frac{n_{e0} B_0 e^2}{\acute{A}\acute{B}\varepsilon_0 m_e \omega_e^2} \partial_x^2 U_{y0},$$
$$W_1 = 1 + \frac{4\Omega_e^2}{\omega_e^2} - \frac{2\Omega_e}{\omega_e^2} \partial_x U_{y0},$$
$$X_1 = 1 + \frac{4\Omega_e^2}{\omega_e^2} - \frac{eB_0}{m_e \omega_e^2} \partial_x U_{y0},$$

$$G_1 = QLiF, \quad G_2 = B_2 iLF + QL\acute{X} + QKiF,$$
$$G_3 = A_2 LFi + B_2 L\acute{X} + B_2 KFi + QL\acute{Y} + QK\acute{X} + RC_2 Fi,$$
$$G_4 = A_2 L\acute{X} + A_2 KFi + B_2 L\acute{Y} + QL\acute{Z} + Q\acute{Y}K + RC_2\acute{X} - RBNiF + PIC_2 Li,$$

$$G_5 = A_2 L\acute{Y} + A_2 K\acute{X} + B_2 L\acute{Z} + B_2 K\acute{Y} + QK\acute{Z} + RC_2\acute{Y} - RBN\acute{X} + PIC_2 Ki - BNLPIi + PIDC_2 L,$$
$$G_6 = A_2 L\acute{Z} + A_2 K\acute{Y} + B_2 K\acute{Z} + RC_2\acute{Z} - RBN\acute{Y} - BNKPIi + PIDC_2 K - PIDBNL,$$
$$G_7 = A_2 K\acute{Z} - RBN\acute{Z} - PIDBNK$$

$$A_2 = MN - QN^2, \quad B_2 = Mi - 2iNQ, \quad C_2 = AN - Bi$$
$$\acute{X} = iG = CF + EF, \quad \acute{Y} = iH + CG + EG, \quad \acute{Z} = CH + EH,$$
$$R = \frac{4T_e i k^2 \alpha n_{e0} e}{m_e \Omega_e^2 \varepsilon_0}, \quad P = \frac{2T_e k e}{m_e \varepsilon_0} \partial_x n_{e0} + \frac{2T_d kd}{m_d \varepsilon_0} \partial_x n_{d0}$$
$$N = \alpha - ikV_{y0}, \quad Q = \frac{2T_i ik}{\acute{Q} m_i \Omega_i^2} \cdot \Lambda,$$

$$M = \frac{Ze\alpha n_{i0}}{\varepsilon_0} + \frac{2T_i Zeik}{m_i\Omega_i\varepsilon_0}\partial_x n_{i0} + \frac{2ikZ^2e^2T_iB_0}{m_i^2\Omega_i^2\varepsilon_0}\partial_x n_{i0} + \frac{2ikn_{i0}Ze}{m_i\Omega_i\varepsilon_0}\partial_x T_i + \frac{2Z^2e^2ikn_{i0}B_0}{m_i^2\Omega_i^2\varepsilon_0}\partial_x T_i + \frac{2ikn_{i0}Ze}{m_i\Omega_i^2\varepsilon_0}\partial_x V_{y0}\partial_x T_i + \Lambda\left[-\frac{2T_i}{\acute{Q}m_i n_{i0}\Omega_i}\partial_x n_{i0} - \frac{2T_iZeB_0}{\acute{Q}m_i^2\Omega_i^2 n_{i0}} - \frac{2}{\acute{Q}m_i}\partial_x T_i - \frac{2ZeB_0}{\acute{Q}m_i^2\Omega_i^2}\partial_x T_i\right],$$

$$\acute{Q} = 1 + \frac{2ZeB_0}{m_i\Omega_i} + \frac{Z^2e^2B_0^2}{m_i^2\Omega_i^2} + \frac{ZeB_0}{m_i\Omega_i^2}\partial_x V_{y0}\partial_x V_{y0},$$

$$L = i + \frac{2T_ek^2}{m_e\Omega_e^2},\quad K = \frac{2T_ek^2\alpha}{m_e\Omega_e^2} - \frac{2T_ek^2ikU_{y0}}{m_e\Omega_e^2} - ikU_{y0} - \alpha,$$

$$J = 2eB_0\Omega_e m_e + 2e^2B_0^2 - 2eB_0m_e\partial_x U_{y0},\quad I = m_e n_{e0}\Omega_e^2,$$

$$H = -ikU_{y0}m_e n_{e0}\Omega_e^2 D + \alpha D m_e n_{e0}\Omega_e^2 - (k^2U_{y0}^2 + \alpha^2) * 2T_ek^2 n_{e0},$$

$$G = -\alpha i m_e n_{e0}\Omega_e^2 + iDm_e n_{e0}\Omega_e^2 - 4T_ek^3 n_{e0}U_{y0} + kU_{y0}m_e n_{e0}\Omega_e^2,$$

$$F = -2T_ek^2 n_{e0} - 2T_dk_d^2 n_{d0} - m_e n_{e0}\Omega_e^2,$$

$$E = \frac{e^2B_0^2 - eB_0m_e\partial_x U_{y0}}{m_e^2\Omega_e},\quad D = -\alpha - ikV_{y0},$$

$$C = \alpha - ikV_{y0},\quad B = ikV_{y0} + \alpha + \frac{2T_iik^3V_{y0}}{m_i\Omega_i^2} - \frac{2T_ik^2\alpha}{m_i\Omega_i^2},$$

$$A = i + \frac{2T_iik^2}{m_i\Omega_i^2} \text{ together with}$$

$$\Lambda = \frac{2Z^2e^2ikn_{i0}B_0}{m_i\Omega_i\varepsilon_0} + \frac{Z^2e^2ikn_{i0}B_0}{m_i\Omega_i^2\varepsilon_0}\partial_x V_{y0} + \frac{2Z_dek_dn_{d0}}{\varepsilon_0}.$$

Conflict of interest statement:
The authors declare that they have no conflict of interest.

References

[1] H. Kakiuchi, H. Ohmi, and K. Yasutake. "Atmospheric-pressure low-temperature plasma processes for thin film deposition". *Journal of Vacuum Science and Technology A: Vacuum, Surfaces and Films*, **32**:030801, 2014.

[2] E. R. Parker, B. J. Thibeault, and M. F. Aimi. "Inductively coupled plasma etching of bulk titanium for MEMS applications". *Journal of the Electrochemical Society*, **152**:C675, 2005.

[3] D. S. Rawal, H. K. Malik, and V. R. Agarwal. "BCl3/Cl2-based inductively coupled plasma etching of GaN/AlGaN using photoresist mask". *IEEE Transactions on Plasma Science*, **40**:2211, 2012.

[4] R. J. Shul, G. B. McClellan, S. A. Casalnuovo, and D. J. Reiger. "Inductively coupled plasma etching of GaN". *Applied Physics Letters*, **69**:1119, 1996.

[5] A. W. Zia, Y. Q. Wang, and S. Lee. "Effect of physical and chemical plasma etching on surface wettability of carbon fiber-reinforced polymer composites for bone plate applications". *Advances in Polymer Technology*, **34**:21480, 2015.

[6] H. Kobayashi. "Behavior of dust particles in plasma etching apparatus". *Japanese Journal of Applied Physics*, **50**:08JE01, 2011.

[7] J. Winter. "Dust in fusion devices-experimental evidence, possible sources and consequences". *Plasma Physics and Controlled Fusion*, **40**:1201, 1998.

[8] J. Li, S. J. Kim, and S. Han. "Characterization of sp2/sp3 hybridization ratios of hydrogenated amorphous carbon films deposited in C2H2 inductively coupled plasmas". *Surface and Coatings Technology*, **422**:127514, 2021.

[9] S. Kumar, A. Malik, D. S. Rawal, S. Vinayak, and H. K. Malik. "Performance analysis of GaN/AlGaN HEMTs passivation using inductively coupled plasma chemical vapour deposition and plasma enhanced chemical vapour deposition techniques". *Defence Science Journal*, **68**:572, 2018.

[10] S. Kumar, D. S. Rawal, and H. K. Malik. "Memory effect in silicon nitride deposition using ICPCVD technique". *Journal of Theoretical and Applied Physics*, **13**:299, 2019.

[11] J. Winter and G. Gebauer. "Dust in magnetic confinement fusion devices and its impact on plasma operation". *Journal of Nuclear Materials*, **266**:228, 1999.

[12] L. Malik and A. Tevatia. "Comparative analysis of aerodynamic characteristics of F16 and F22 combat aircraft using computational fluid dynamics". *Defence Science Journal*, **71**:137, 2021.

[13] A. K. Aria and H. K. Malik. "Studies on waves and instabilities in a plasma sheath formed on the outer surface of a space craft". *Physics of Plasmas*, **15**:043501, 2008.

[14] L. Malik, S. Rawat, M. Kumar, and A. Tevatia. "Simulation studies on aerodynamic features of Eurofighter Typhoon and Dassault Rafale combat aircraft". *Materials Today: Proceedings*, **38**:191, 2021.

[15] V. V. Zhurin, H. R. Kaufman, and R. S. Robinson. "Physics of closed drift thrusters". *Plasma Sources Science and Technology*, **8**:R1, 1999.

[16] T. Burton, A. M. Schinder, G. Capuano, J. J. Rimoli, M. L. R. Walker, and G. B. Thompson. "Plasma-induced erosion on ceramic wall structures in Hall-effect thrusters". *Journal of Propulsion and Power*, **30**:690, 2014.

[17] S. Singh and H. K. Malik. "Growth of low-frequency electrostatic and electromagnetic instabilities in a Hall thruster". *IEEE Transactions on Plasma Science*, **39**:1910, 2011.

[18] S. Singh, H. K. Malik, and Y. Nishida. "High frequency electromagnetic resistive instability in a Hall thruster under the effect of ionization". *Physics of Plasmas*, **20**:102109, 2013.

[19] H. K. Malik and S. Singh. "Resistive instability in a Hall plasma discharge under ionization effect". *Physics of Plasmas*, **20**:52115, 2013.

[20] A. Lazurenko, V. Vial, M. Prioul, and A. Bouchoule. "Experimental investigation of high-frequency drifting perturbations in Hall thrusters". *Physics of Plasmas*, **12**:13501, 2005.

[21] A. Kapulkin and M. M. Guelman. "Low-Frequency Instability in Near-Anode Region of Hall Thruster". *IEEE Transactions on Plasma Science*, **36**:2082, 2008.

[22] S. Barral, K. Makowski, Z. Peradzyński, and M. Dudeck. "Transit-time instability in Hall thrusters". *Physics of Plasmas*, **12**:73504, 2005.

[23] S. Chable and F. Rogier. "Numerical investigation and modeling of stationary plasma thruster low frequency oscillations ". *Physics of Plasmas*, **12**:33504, 2005.

[24] E. Chesta, C. M. Lam, N. B. Meezan, D. P. Schmidt, and M. A. Cappelli. "A characterization of plasma fluctuations within a Hall discharge". *IEEE Transactions on Plasma Science*, **29**:582, 2001.

[25] J. B. Parker, Y. Raitses, and N. J. Fisch. "Transition in electron transport in a cylindrical Hall thruster". *Applied Physics Letters*, **97**:91501, 2010.

[26] W. Frias, A. I. Smolyakov, I. D. Kaganovich, and Y. Raitses. "Long wavelength gradient drift instability in Hall plasma devices. I. Fluid theory". *Physics of Plasmas*, **19**:72112, 2012.

[27] A. I. Smolyakov, Y. Raitses W. Frias, and N. J. Fisch. "Gradient instabilities in Hall thruster plasmas". *The 32nd International Electric Propulsion Conference, Wiesbaden, Germany*, , 2011.

[28] M. Starodubtsev, M. Kamal-Al-Hassan, H. Ito, N. Yugami, and Y. Nishida. "Low-frequency sheath instability in a non-Maxwellian plasma with energetic ions". *Physical Review Letters*, **92**:45003, 2004.

[29] L. Malik, M. Kumar, and I. V. Singh. "A three-coil setup for controlled divergence in magnetic nozzle". *IEEE Transactions on Plasma Science*, **49**:2227, 2021.

[30] L. Malik. "Tapered coils system for space propulsion with enhanced thrust: a concept of plasma detachment". *Propulsion and Power Research*, **11**:171, 2022.

[31] L. Malik. "Novel concept of tailorable magnetic field and electron pressure distribution in a magnetic nozzle for effective space propulsion". *Propulsion and Power Research*, **12**:59, 2023.

[32] L. Malik. "In-flight Plume Control and Thrust Tuning in Magnetic Nozzle using Tapered-coils System under the Effect of Density Gradient". *IEEE Transactions on Plasma Science*, **51**:1325, 2023.

[33] H. K. Malik. *Laser-Matter Interaction for Radiation and Energy*. CRC Press, 2021.

[34] H. K. Malik, J. Tyagi, and D. Sharma. "Growth of Rayleigh instability in a Hall thruster channel having dust in exit region". *AIP Advances*, **9**:055220, 2019.

[35] J. Tyagi, D. Sharma, and H. K. Malik. "Discussion on Rayleigh equation obtained for a Hall thruster plasma with dust". *Journal of Theoretical and Applied Physics*, **12**:227, 2018.

[36] J. Tyagi, S. Singh, and H. K. Malik. "Effect of dust on tilted electrostatic resistive instability in a Hall thruster". *Journal of Theoretical and Applied Physics*, **12**:39, 2018.

[37] L. Malik, G. S. Saini, and A. Tevatia. *A Self-sustained Machine Learning Model to Predict the In-flight Mechanical Properties of a Rocket Nozzle by Inputting Material Properties and Environmental Conditions*. Handbook of Sustainable Materials: Modelling, Characterization, and Optimization, CRC Press, 2023.

[38] L. Malik, G. S. Saini, and A. Tevatia. *Sustainability of Wind Turbine Blade: Instantaneous Real-Time Prediction of Its Failure Using Machine Learning and Solution Based on Materials and Design*. Handbook of Sustainable Materials: Modelling, Characterization, and Optimization, CRC Press, 2023.

[39] Munish, R. Dhawan, R. Kumar, and H. K. Malik. "Density gradient driven instability in an E×B plasma system having temperature gradients ". *Journal of Taibah University for Science*, **16**:725, 2022.

[40] Munish, R. Dhawan, D. Sharma, and H. K. Malik. "Influence of magnetic field and ionization on gradient driven instability in an $\mathbf{E} \times \mathbf{B}$ plasma". *Journal of Agricultural Science*, **92**:499–503, 2022.

[41] L. Malik, A. Escarguel, M. Kumar, A. Tevatia, and R. S. Sirohi. "Uncovering the remarkable contribution of lasers peak intensity region in holography". *Laser Physics Letters*, **18**:086003, 2021.

[42] L. Malik and A. Escarguel. "Role of the temporal profile of femtosecond lasers of two different colours in holography". *Europhysics Letters*, **124**:64002, 2019.

[43] L. Malik. "Dark hollow lasers may be better candidates for holography". *Optics and Laser Technology*, **132**:106485, 2020.

[44] K. Singh, V. Kumar, and H. K. Malik. "Electron inertia contribution to soliton evolution in an inhomogeneous weakly relativistic two-fluid plasma". *Physics of Plasmas*, **12**:072302, 2005.

[45] H. K. Malik. "Ion acoustic solitons in a relativistic warm plasma with density gradient". *IEEE Transactions on Plasma Science*, **23**:813, 1995.

[46] H. K. Malik and K. Singh. "Small amplitude soliton propagation in a weakly relativistic magnetized space plasma: electron inertia contribution". *IEEE Transactions on Plasma Science*, **33**:1995, 2005.

[47] H. K. Malik. "Ion acoustic solitons in a weakly relativistic magnetized warm plasma". *Physical Review E*, **54**:5844, 1997.

[48] R. Kumar, H. K. Malik, and K. Singh. "Effect of dust charging and trapped electrons on nonlinear solitary structures in an inhomogeneous magnetized plasma". *Physics of Plasmas*, **19**:012114, 2012.

[49] H. K. Malik, R. Tomar, and R. P. Dahiya. "Conditions for reflection and transmission of an ion acoustic soliton in a dusty plasma with variable charge dust". *Physics of Plasmas*, **21**:072112, 2014.